TUYỂN TẬP BÁO CÁO HỘI NGHỊ TOÀN QUỐC

KHOA HỌC TRÁI ĐẤT VÀ TÀI NGUYÊN VỚI PHÁT TRIỂN BỀN VỮNG

Hà Nội, 12 - 11 - 2020

ERSD 2020



NHÀ XUẤT BẢN GIAO THÔNG VẬN TẢI

Non-linear filtering algorithms for kinematic positioning on the application of maritime navigation

Dung Trung Pham,†
Hanoi University of Mining and Geology, Vietnam

ABSTRACT

In the field of kinematic positioning applied for maritime navigation, a vessel is often tracked by low-cost sensors, which are lightweight, small size, and low in price, but instability and low accuracy. The non-linearity is one of the most difficult characteristics in the estimation, and it is contributed by highly non-linear functions of both the kinematic model and the observation model as well as the measurement error. To overcome this problem, a suitable non-linear filtering algorithm needs to be selected. In this paper, a scenario of maritime navigation is given, in which the sensor's measurement used for tracking the vessel is simulated by the Monte Carlo method. Two non-linear filtering algorithms consisting of extended Kalman filter (EKF) and particle filter (PF) is applied since these algorithms are appropriated to different levels of non-linearity. The position accuracy of these algorithms is determined in cases of varying measurement accuracy and observation geometry. The main result of this work is that the improvement in accuracy between PF and EKF is investigated on the wide range of non-linearity. Based on this information about the improvement, the users can choose a suitable algorithm to deal with the mentioned non-linearity problem for their applications.

Keywords: Non-linear filtering algorithms; Kinematic positioning; Maritime navigation.

Introduction

Non-linear estimation problem has long constituted an attractive topic for researchers. The non-linearity is one of the most difficulties in estimation by filtering algorithms. In the kinematic positioning, the non-linearity is often conducted by both the system and the observation models, which are non-linear equations. In addition, the high measurement errors from measurements and bad observation geometry are also the main reasons of high non-linearity. Several filtering algorithms had proposed to deal with this issue. EKF, one of the most widely used algorithms, can deal with this problem. EKF is extended straightforwardly from the Kalman filter (KF) (Kalman 1960), in which the linear approximation technique is used by the Taylor series expansion (Gelb 1979). Fast computational time is the main advantage of this filter. However, the linear approximation is not satisfactory for highly non-linear models, which leads to the divergent phenomenon of EKF (Niu, Varshney et al. 2008). Hence this algorithm is only suitable for weak non-linearity. To overcome this problem, PF (Gordon, Salmond et al. 1993) is the most suitable algorithm to apply in these cases. In this filter, mean and covariance quantities are approximated directly from a large number of random sample points. This algorithm can also cope with non-Gaussian noise distribution, but the burden in computational time is expensive (Karlsson, Schön et al. 2005). From these analyses, both the above algorithms have advantages and disadvantages in terms of accuracy and computational time. The selection of an appropriate algorithm between the above-mentioned algorithms will focus on the accuracy taken the computational time into account. In this study, the improvement in accuracy is considered as the main parameter for choosing algorithms. In theory, the PF is better than EKF due to high non-linearity, but the quantity in the improvement of PF compared to EKF depends also on parameters of scenarios. Hence, in this paper, this improvement will be investigated for a certain application of maritime navigation. The paper is organized in four following sections. A brief theory about filtering algorithms including EKF and PF is described in section 2. Section 3 presents a vessel positioning in the maritime application. The results of determination on the improvement in the accuracy according to varying both the measurement accuracy and the observation geometry are discussed

† *Tác giả liên hệ*
Email: phamtrungdung@humg.edu.vn

in section 3. The main findings, limitations are given in section 4. Finally, conclusions and future works are presented in section 5.

2. Filtering algorithms

2.1. Extended Kalman filter

EKF is the most widely used in the non-linear estimation. The main concept of this algorithm was proposed by Schmidt (1966). The method was also well-known as the Kalman-Schmidt filter.

If the state vector $\boldsymbol{y}$ is passed through the prediction model $\boldsymbol{\phi}$ and the observation model $\boldsymbol{\theta}$:

$$\bar{\boldsymbol{y}}_{k+1} = \boldsymbol{\phi}(\hat{\boldsymbol{y}}_k, \boldsymbol{\xi}_k), \tag{1}$$

$$\bar{\boldsymbol{l}}_{k+1} = \boldsymbol{\theta}(\bar{\boldsymbol{y}}_{k+1}, \boldsymbol{\eta}_k), \tag{2}$$

then the procedure of the EKF can be presented in Fig. 1.

2.2. Particle filter

The particle filter (PF) is widely employed for non-linear and non-Gaussian models. The central idea of the PF is to approximate the posterior PDF of the state vector as a set of random samples. The mean and covariance can be obtained from a precise posterior PDF, which is generated by a great number of samples. This method is known under the names of the bootstrap method, condensation algorithm (Isard and Blake 1998), and sequential Monte Carlo. The first paper on the sequential MC method was presented by Hammersley and Morton (1954). However, the PF began to be commonly used with the seminal paper of Gordon, Salmond et al. (1993). Here, resampling, an important step, is introduced, which created a novel method, known as sampling importance resampling (SIR) or particle filter. In the scope of this study, PF theory based on the SIR algorithm will be described below.

A posterior PDF of the predicted state vector $\boldsymbol{y}_{k+1}$, $p(\boldsymbol{y}_{k+1}|\boldsymbol{L}_k)$, can be determined by using a probability model of state evolution $p(\boldsymbol{y}_{k+1}|\boldsymbol{y}_k)$, as follows:

$$p(\boldsymbol{y}_{k+1}|\boldsymbol{L}_k) = \int p(\boldsymbol{y}_{k+1}|\boldsymbol{y}_k)p(\boldsymbol{y}_k|\boldsymbol{L}_k)d\boldsymbol{y}_k, \tag{3}$$

where $\boldsymbol{L}_k$ denotes the set of all observations received up to and including $\boldsymbol{l}_k$: $\boldsymbol{L}_k = \{\boldsymbol{l}_i, i = 1,2,\dots,k\}$; and a filtering probability density $p(\boldsymbol{y}_k|\boldsymbol{L}_k)$ for the Bayesian inference is given by:

$$p(\boldsymbol{y}_k|\boldsymbol{L}_k) = \frac{p(\boldsymbol{l}_k|\boldsymbol{y}_k)p(\boldsymbol{y}_k|\boldsymbol{L}_{k-1})}{p(\boldsymbol{l}_k|\boldsymbol{L}_{k-1})}. \tag{4}$$

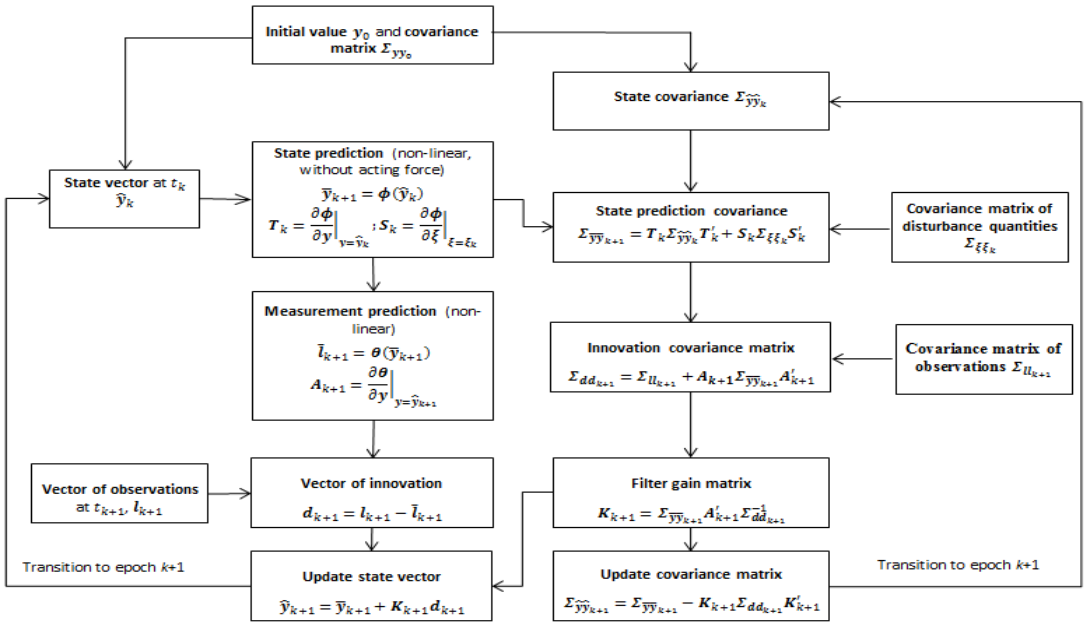


Fig. 1 Scheme of EKF for non-linear estimation, in which the subscript k indicates a value at time t_k; $\boldsymbol{T}_k$ is transition matrix; $\boldsymbol{S}_k$ is matrix of disturbance quantities; and $\boldsymbol{\xi}_k$ is the vector of Gaussian process noise ($E[\boldsymbol{\xi}_k] = 0$); $\boldsymbol{A}_{k+1}$ is design matrix; and $\boldsymbol{\eta}_k$ is the vector of Gaussian observation noise ($E[\boldsymbol{\eta}_k] = 0$).

The PF approximates the probability density function $p(\boldsymbol{y}_k|\boldsymbol{L}_k)$ by a significant number of N_{PF} independent particles $\boldsymbol{y}_{k,i}$, $i=1,2,\ldots N_{PF}$, and their associated weights $W_{k,i}$, $i=1,2,\ldots N_{PF}$, where the sum of all weights is proportional to unity. The PF updates the state vector and the corresponding weights recursively with each new measurement. In (4), the normalization factor $p(\boldsymbol{l}_k|\boldsymbol{L}_{k-1})$ is usually unknown. However, this factor is not essential for this method, since the probability density function $p(\boldsymbol{y}_k|\boldsymbol{L}_k)$, can be sufficiently evaluated by:

$$p(\boldsymbol{y}_{k+1}|\boldsymbol{L}_k) \propto p(\boldsymbol{l}_k|\boldsymbol{y}_k)p(\boldsymbol{y}_k|\boldsymbol{L}_{k-1}), \tag{5}$$

In theory, a Monte Carlo method can be used to approximate the uncertainty of arbitrary probability density functions. However, in this study, only the Gaussian distribution is used. The likelihood function $p(\boldsymbol{l}_k|\boldsymbol{y}_k)$ is computed by considering the measurement standard deviation (STD) σ under the assumption of a Gaussian distribution:

$$p(\boldsymbol{l}_k|\boldsymbol{y}_k) = \frac{1}{\sqrt{2\pi}\sigma} e^{-\frac{(l_k - y_k)^2}{2\sigma^2}} \tag{6}$$

and $p(\boldsymbol{y}_k|\boldsymbol{L}_{k-1})$ is approximated with particles which are known to constitute the main idea of the PF method, according to:

$$p(\boldsymbol{y}_k|\boldsymbol{L}_{k-1}) \approx \frac{1}{N_{PF}} \sum_{i=1}^{N_{PF}} \delta(\boldsymbol{y}_k - \boldsymbol{y}_{k,i}), \tag{7}$$

where $\delta(\cdot)$ is the delta-Dirac function.

However, this approach suffers from divergence phenomena, in which almost all of the particles' weights have a value of 0, except one non-zero weight, after a few steps. This problem can be handled by a resampling step. Several resampling algorithms were analyzed and compared by Hol, Schön et al. (2006). The SIR algorithm is briefly described by the following procedure:

Step 1: N_{PF} particles $\boldsymbol{y}_{0,i}$, $i=1,2,\ldots, N_{PF}$ are drawn depending on the Gaussian distribution $p(\boldsymbol{y}_0)$ at time $t_k = 0$.

Step 2: The weights $W_{k,i} = p(\boldsymbol{l}_k|\boldsymbol{y}_{k,i})$ are calculated by (6), and normalised weights can be defined as:

$$\widetilde{W}_{k,i} = \frac{W_{k,i}}{\sum_{j=1}^{N_{PF}} W_{k,j}}, \; i = 1,2,\ldots,N_{PF}. \tag{8}$$

Step 3: A new set of particles $\boldsymbol{y}^*_{k,i}$, $i=1,2,\ldots, N_{PF}$ are rearranged from the current set $\boldsymbol{y}_{k,i}$, $i=1,2,\ldots, N_{PF}$ by the resampling method (Karlsson and Gustafsson 2001).

Step 4: At time t_{k+1}, new particles $\boldsymbol{y}_{k+1,i}$, $i=1,2,\ldots, N_{PF}$ are drawn, which are based on the function (1) as:

$$\boldsymbol{y}_{k+1,i} = \boldsymbol{\phi}(\boldsymbol{y}^*_{k,i}, \boldsymbol{\xi}_{k,i}), i = 1,2,\ldots,N_{PF}. \tag{9}$$

where the process noise $\boldsymbol{\xi}_{k,i}$ is simulated by a Gaussian distribution.

Step 5: Increase time $t_k := t_{k+1}$ and repeat from step 2.

3. Application to maritime navigation

3.1. Scenario

The case study is investigated on the maritime application. Whereby, a vessel is tracked by two coastal radars located at the reference points (X_1, Y_1) and (X_2, Y_2), respectively in Fig. 2. These radars are to provide simultaneously two distances s_1 and s_2 each Δt second, and the vessel is tracked during τ second. In this scenario, suppose that the vessel moves from the west to the east in the *x-y* plane with a constant velocity *v*, and the position of the vessel is determined in a good weather condition, such that external influences such as wind, current, and wave are trivial, and they can be ignored in the computation.

3.2 Modeling for the prediction and observation steps

This state vector is propagated through two processes of the time update and measurement update, which corresponds to the system model and the observation model of an estimation algorithm. The goal of the system model is to propagate the state vector forward in time and to determine how this vector varies with time. The straight linear model is a simplification of the movement of the vessel in its trajectory in reality.

In the plane, it is assumed that the vessel moves on the straight line between two points with a constant velocity, and the measuring epochs are realized at these points.

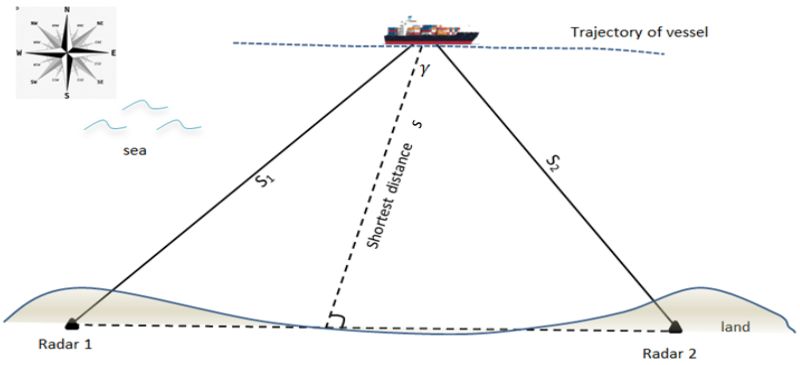


Fig. 2. A vessel is tracked by two distance measurements provided by costal radars.

The geometric model between two consecutive epochs from *k* to *k+1* is illustrated as (Aussems 1999):

$$\begin{aligned} \bar{x}_{k+1} &= \hat{x}_k + \hat{v}_{k+1} \cdot \Delta t \cdot \cos(\hat{\varphi}_k + \Delta\bar{\varphi}_{k+1}) \\ \bar{y}_{k+1} &= \hat{y}_k + \hat{v}_{k+1} \cdot \Delta t \cdot \sin(\hat{\varphi}_k + \Delta\bar{\varphi}_{k+1}) \\ \bar{\varphi}_{k+1} &= \hat{\varphi}_k + \Delta\bar{\varphi}_{k+1} \\ \bar{v}_{k+1} &= \hat{v}_k \\ \Delta\bar{\varphi}_{k+1} &= \Delta\hat{\varphi}_k \end{aligned} \tag{10}$$

Where *x* and *y* are coordinates in the horizontal plane, φ is the orientation, *v* is the velocity, and $\Delta\varphi$ is orientation change of the vessel.

The observation model is to update the state vector with a set of measurements and to identify how measurements vary with the state vector. The distance, a highly non-linear model with respect to the state vector, is used for modeling radars' measurements. The observation vector of two distances in the mentioned scenario at epoch *k* can then be expressed by:

$$\boldsymbol{l}_k = (s_{1,k} \quad s_{2,k})', \tag{11}$$

Where $s_{1,k}$ and $s_{2,k}$ are used by the equations:

$$s_k = \sqrt{(x_k - X_o)^2 + (y_k - Y_o)^2}, \tag{12}$$

With (X_0, Y_0) and (x_k, y_k) are known and unknown coordinates of the radar and the vessel, respectively at epoch *k*.

4. Results

To evaluate the ability of these above algorithms, the position accuracy is used and it is computed by the root mean square error RMSE as:

$$RMSE = \sqrt{\frac{\sum_{k=0}^{N}((\tilde{x}_{k+1} - \hat{x}_{k+1})^2 + (\tilde{y}_{k+1} - \hat{y}_{k+1})^2)}{N}}, \tag{13}$$

Where *N* is the number of measuring epochs; $\tilde{x}$ and $\tilde{y}$ are the north and east coordinates, respectively, of the true trajectory; and $\hat{x}$ and $\hat{y}$ are the estimations of corresponding coordinates by the filtering algorithm.

The improvement in accuracy of PF relative to EKF is calculated by both absolute and relative proportions as:

$$\Delta RMSE = RMSE_{EKF} - RMSE_{PF} \tag{14}$$

$$\%RMSE = \frac{(RMSE_{EKF} - RMSE_{PF})}{RMSE_{PF}} \cdot 100\%, \tag{15}$$

Where $RMSE_{EKF}$ and $RMSE_{PF}$ are the position accuracy estimated by EKF and PF, respectively.

In this study, the measurement accuracy and observation geometry are the main factors influencing straightforwardly on the position accuracy. However, the quantity of position accuracy depends also on the parameters of scenarios. Hence, the rest of the paper will investigate the influence of the position

accuracy with changing measurement accuracy and the observation geometry, in which the scenario in section 3.1 is used by the given parameters in table 1.

Table. 1. Parameters of scenario for tracking the vessel.

Parameters	Denotations	Quantities
Velocity, sampling time, and total time	v, Δt, τ	5 m/s^2, 1 s, and 100 s
STD of acceleration and rotational rate	σ_{a_ξ}, σ_{φ_ξ}	0.01 m/s^2, 0.01 rad/s^2
STD of distance measurement	σ_s	4 m ÷ 40 m
Horizontal position of radar 1	(X_1,Y_1)	(100 m, 100 m)
Horizontal position of radar 2	(X_2,Y_2)	(100 m, 600 m)

Both process noise and measurement noise corresponding given quantities in table 1 are assumed to be Gaussian. The initial state vector is based on one-point initialization. The initial state vector is the first observed position, orientation, velocity, and orientation change $\boldsymbol{y}_0$ = (1100 m, 100 m, 90^o, 1 m/s, 0.01^o)'. The covariance matrix of the initial state vector is $\boldsymbol{\Sigma}_{\boldsymbol{yy}_0} = diag((10\,m)^2 \quad (10\,m)^2 \quad (1^o)^2 \quad (1\,m/s)^2 \quad (0.1^o)^2)$. To obtain reliable results in accuracy, the number of particles using PF, N_{PF} = 3×10^4.

In the first evaluation, measurement accuracy is one of the main factors affecting the position accuracy. The position accuracy will investigate according to varying the measurement accuracy in the range [4 m, 40 m] in ten equal intervals while the observation geometry remains unchanged by s =1 km. The estimated accuracy of EKF and PF determined by the averaged value of position RMSE over 100 epochs is shown in Fig. 3 (a).

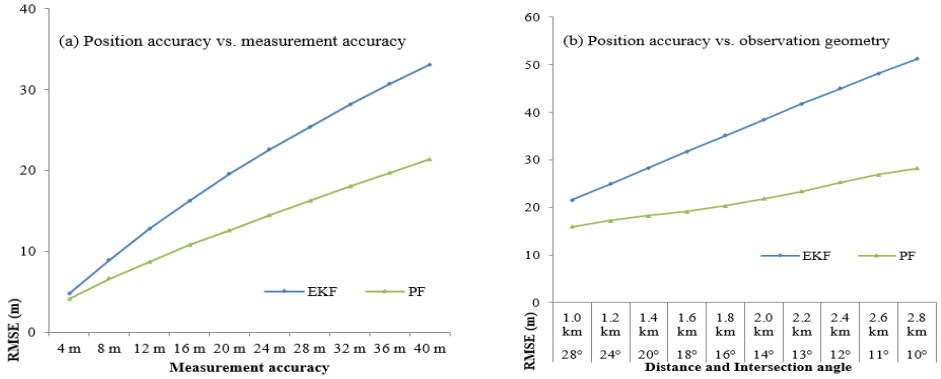


Fig. 3. Position RMSEs obtained by EKF and PF versus measurement accuracy (a) and observation geometry (b).

According to accuracy, the RMSE values of these two algorithms increase with increasing measurement accuracy. The RMSE of PF is the smallest than that of EKF for the whole interval of surveyed measurement accuracy. Similar results are discussed in Konatowski, Kaniewski et al. (2016) and Doucet, Freitas et al. (2001). Besides, the important aspect of this evaluation is the improvement in the accuracy of PF compared to EKF. Both absolute and relative proportions of the improvement are computed by equation (14) and (15), respectively, and listed in Table 2. PF achieves approximately from 6% to 48% or from 0.3 m to 20 m higher in position RMES than that of EKF when STD of measurement increases from 4 m to 40 m. These results indicate that the improvement in PF becomes larger in the case of low measurement accuracy, but these improvement values are only slightly different in the case of high measurement accuracy. These results are consistent with the analysis of bearing-only tracking for the maneuvering case (Ristic, Arulampalam et al. 2004).

Table 2. Comparison in the accuracy performance between EKF and PF due to varying measurement accuracy.

σ_s (m)	ΔRMSE (m)	%RMSE	σ_s (m)	ΔRMSE (m)	%RMSE
4	0.308	6 %	24	7.159	40 %
8	1.908	24 %	28	8.469	42 %
12	3.511	34 %	32	9.894	45 %
16	4.650	35 %	36	11.015	46 %
20	5.750	37 %	40	12.334	48 %

In the second evaluation, the observation geometry is considered as another factor affecting the position accuracy of the vessel. In this evaluation, the observation geometry is changed by the shortest distance *s* between two stationary radars and the vessel or the intersection angle γ (see Fig. 2) while the measurement accuracy is unchanged by $\sigma_s = 1^o$. To avoid divergence phenomenon of filtering algorithms due to high non-linearity, the shortest distance *s* is varied from 1.0 km to 2.8 km in 10 equal intervals or the intersection angle decreases from 28^o to 10^o. The position RMSEs of these algorithms averaged over 100 epochs are shown in Fig 3(b). The position RMSE of these algorithms increases with increasing value of the shortest distance *s* or decreasing value of intersection angle γ. Similar to analyses according to a variation on the measurement accuracy, the PF obtains higher RMSE than that of EKF. The improvement in accuracy of PF compared to EKF also increases with increasing value of the shortest distance, as summarized in Table 3. The relative improvements in PF rise from 28% to 64%. Similarly, the absolute improvements increase between approximately 5.5 m and 23 m. These results are in agreement with the theory about geometrical configuration. The change in RMSE of these algorithms is due to geometrical reasons. Since the intersection angle γ decreases in the above-mentioned range that leads to bad geometry (Atkinson 1989). Similar results in the context of unmanned aerial vehicle navigation (UAV) can be found in Veth (2013). Note that although certain observation geometry will optimize tracking performance in terms of position accuracy, this subject of the optimization of geometry is not in the scope of this research.

Table 3. Comparison in the accuracy performance between EKF and PF due to varying observation geometry.

s (km)	γ	ΔRMSE (m)	%RMSE	*s* (km)	γ	ΔRMSE (m)	%RMSE
1.0	28°	5,583	28 %	2.0	14°	16,257	58 %
1.2	24°	7,722	36 %	2.2	13°	17,950	59 %
1.4	20°	10,079	45 %	2.4	12°	19,674	61 %
1.6	18°	12,612	53 %	2.6	11°	21,351	62 %
1.8	16°	14,572	57 %	2.8	10°	22,983	64 %

Other non-linear filtering algorithms, such as the ensemble KF, unscented KF, and Gauss filter should be also investigated to deal with this problem. Furthermore, other parameters such as velocity, sampling time, which can influence the position accuracy, do not investigate in this study. Due to the limitation in the length of this paper, the comparison of the computational time of EKF and PF did not present here, but it can be seen in Pham and Schwieger (2016) and Hol (2004).

5. Conclusions

There has little doubt that the assessment of the ability of a filtering algorithm suffering from non-linearity is an important issue. The main finding of this study is that the improvement in the position accuracy of PF compared to EKF is computed according to various levels of non-linearities. The difference in non-linearity is due to the varying parameters of the measurement accuracy and the observation geometry in their wide ranges. Regarding weak non-linearity, when the measurement accuracy is high or the observation geometry is good, the improvement in accuracy of PF compared to EKF is not important. It means that EKF is the optimal choice in this case. In contrast, for high non-linearity when the measurement accuracy is low or the observation geometry is bad, this improvement is considerable. It means that PF is the best choice. So, the improvement can be used as an important parameter in the selection of filtering algorithms. A chosen suitable filtering algorithm can be solved well with the mentioned non-linearity problem.

In future work, other non-linear filtering algorithms should be investigated to cope with different levels of non-linearity. A potential solution for this problem is that an algorithm mixed between EKF and PF, which can meet the requirement in estimated accuracy but reduce computational time, should be applied (Schön, Gustafsson et al. 2005). Moreover, the non-linearity can be considered as an alternative parameter to select an appropriate algorithm.

References

Atkinson, K. (1989). An Introduction to Numerical Analysis. Québec, Canada, *John Wiley & Sons*, Inc.

Aussems, T. (1999). " Positionsschätzung von Landfahrzeugen mittels Kalman-Filterung aus Satelliten- und Koppelnavigationsbeobachtungen." Veröffentlichung des Geodätischen Instituts der Rheinisch-*Westfälischen Technischen Hochschule Aachen* Nr. 55.

Doucet, A., N. d. Freitas and N. Gordon (2001). Sequential Monte Carlo Methods in Practice, New York: Springer-Verlag.

Gelb, A. (1979). Applied optimal estimation. Massachusetts, USA., *The M.I.T press*.

Gordon, N. J., D. J. Salmond and A. F. M. Smith (1993). Novel approach to nonlinear/non-Gaussian Bayesian state estimation. *IEE Proceedings-F*.

Hammersley, J. M. and K. W. Morton (1954). "Poor man's Monte Carlo." Journal of the Royal Statistical Society, *Series B (Statistical Methodology)* 16: 23-38.

Hol, J. D. (2004). Resampling in Particle filters. SE-581 83 Linköping, Sweden, *Department of Electrical Engineering*.

Hol, J. D., T. B. Schön and F. Gustafsson (2006). On Resampling Algorithms for Particle Filters. *2006 IEEE Nonlinear Statistical Signal Processing Workshop*. Cambridge: 79-82.

Isard, M. and A. Blake (1998). "Condensation-conditional Density Propagation for Visual Tracking." *International Journal of Computer Vision* 29(1): 5-28.

Kalman, R. E. (1960). "A New Approach to Linear Filtering and Prediction Problems." *Basic Engineering* 82(1): 35-45.

Karlsson, R. and R. Gustafsson (2001). Range estimation using angle-only target tracking with particle filters. *Proceedings of the 2001 American Control Conference*, Arlington, VA, USA, USA.

Karlsson, R., T. Schön and F. Gustafsson (2005). "Complexity Analysis of the Marginalized Particle Filter." *IEEE Transactions on Signal Processing* 53(11): 4408-4411.

Konatowski, S., P. Kaniewski and J. Matuszewski (2016). "Comparison of Estimation Accuracy of EKF, UKF and PF filters." *Annual of navigation* 23(1): 69-87.

Niu, R., P. K. Varshney, M. Alford, A. Bubalo, E. Jones and M. Scalzo (2008). "Curvature nonlinearity measure and filter divergence detector for nonlinear tracking problems." in Proc. Int. Conf. Inf. *Fusion, Cologne*, Germany, Jun.-Jul.

Pham, D. and V. Schwieger (2016). Comparison of Filtering Algorithms in Vehicle Positioning by Using Low-Cost Sensors. *International Conference on Machine Control & Guidance*. Vichy, France.

Ristic, B., S. Arulampalam and N. Gordon (2004). Beyond the Kalman Filter. Boston, London, *Artech House*.

Schön, T., F. Gustafsson and P. Nordlund (2005). "Marginalized particle filter for nonlinear state-space model." *IEEE Transactions on Signal Processing* 53: 2279-2289.

Veth, M. J. (2013). "Nonlinear Estimation Techniques for Navigation." Navigation Sensors and Systems in GNSS Degraded and Denied Environments, *NATO STO lecture series SET*-197.

TÓM TẮT

Phép lọc phi tuyến cho định vị động ứng dụng trong định vị hàng hải

Phạm Trung Dũng
Trường Đại học Mỏ- Địa chất Hà Nội, Việt Nam

Trong lĩnh vực định vị động ứng dụng trong định vị hàng hải, vị trí của tàu thường được theo dõi bởi các cảm biến giá rẻ với đặc điểm như trọng lượng nhẹ, kích thước nhỏ, và giá thấp nhưng kém ổn định và độ chính xác thấp. Mức độ phi tuyến là một trong những đặc tích phức tạp nhất trong bài toán ước lượng và nó phụ thuộc vào hàm phi tuyến của mô hình hệ thống và mô hình trị đo cùng với sai số đo. Để giải quyết vấn đề này, thuận toán lọc phù hợp cần phải được lựa chọn. Trong bài báo này, một kịch bản trong định vị hàng hải được giả định, trong đó trị đo bằng cảm biến sử dụng cho định vị tàu được mô phỏng bởi phương pháp Monte Carlo. Hai thuật toán lọc phi tuyến bao gồm phép lọc Kalman mở rộng (Extended Kalman filter) và lọc hạt (Particle filter) được áp dụng bởi vì các thuật toán này phù hợp với các mức độ phi tuyến tính khác nhau. Độ chính xác vị trí của những thuật toán này được xác định trong trường hợp thay đổi về sai số đo và đồ hình hình học. Kết quả chính của bài báo là mức độ cải thiện về độ chính xác giữa hai thuật toán trên được điều tra với thay đổi lớn về mức độ phi tuyến tính. Dựa vào thông tin về mức độ cải thiện độ chính xác có thể lựa chọn được thuật toán phù hợp để giải quyết vấn đề phi tuyến tính trong định vị động.

Từ khóa: lọc phi tuyến tính; định vị động; định vị hàng hải.

KHOA HỌC TRÁI ĐẤT VÀ TÀI NGUYÊN VỚI PHÁT TRIỂN BỀN VỮNG



ISBN 978-604762277-1